

A Model for the Inhibition of Urease by Hydroxamates

Ann J. Stemmler,[†] Jeff W. Kampf,[†] Martin L. Kirk,^{*,‡} and Vincent L. Pecoraro^{*,‡}

Departments of Chemistry, University of Michigan
Ann Arbor, Michigan 48109-1055
The University of New Mexico
Albuquerque, New Mexico 87131-1096

Received February 13, 1995

Urease catalyzes the decomposition of urea to ammonium and carbamate ions using an active site that requires two nickel(II) atoms per protein subunit.¹ A variety of spectroscopic data has been obtained in order to elucidate the structure of the urease enzyme.² More recently an X-ray structure of urease shows that the two Ni ions are linked by a bridging carbamate and that two imidazole nitrogen atoms are bound to each nickel. Another carboxylate and a bound solvent fill the remaining coordination sites of the Ni.³ Variable temperature magnetic susceptibility data and MCD spectra have provided conflicting results for magnetic exchange interactions.⁴ Magnetic susceptibility and variable temperature MCD data of the competitive inhibitor β -mercaptoethanol bound to urease show that the Ni ions are strongly antiferromagnetically exchange coupled.^{4a} The enzyme is also inhibited by hydroxamic acids.⁵ In particular, biphasic inhibition has been observed with acetohydroxamic acid, and a model for a structural conversion, shown as Scheme 1, has been proposed to explain this observation.⁶ We provide here the crystal structure and variable temperature magnetic susceptibility of a nickel dimer which reveals an alternative description for the mechanism of inhibition of urease by hydroxamic acids.

[†] University of Michigan.

[‡] The University of New Mexico.

(1) Andrews, R. K.; Blakeley, R. L.; Zerner, B. *The Bioinorganic Chemistry of Nickel*; VCH Publishers: New York, 1988; pp 141–165.

(2) (a) Hausinger, R. P. *Biochemistry of Nickel*; Plenum Press: New York, 1993; Vol. 12, pp 23–50. (b) Kolodziej, A. F. In *Progress in Inorganic Chemistry*; Karlin, K. D., Ed.; John Wiley & Sons, Inc.: New York, 1994; Vol. 41, pp 493–580.

(3) Jabri, E.; Carr, M. B.; Hausinger, R. P.; Karplus, P. A. *Science*, in press.

(4) (a) Clark, P. A.; Wilcox, D. E. *Inorg. Chem.* **1989**, *28*, 1326–1333. (b) Finnegan, M. G.; Kowal, A. T.; Werth, M. T.; Clark, P. A.; Wilcox, D. E.; Johnson, M. K. *J. Am. Chem. Soc.* **1991**, *113*, 4030–4032. (c) Day, E. P.; Peterson, J.; Sendova, M. S.; Todd, M. J.; Hausinger, R. P. *Inorg. Chem.* **1993**, *32*, 634–638.

(5) (a) Kobashi, K.; Kumaki, K.; Hase, J. *Biochim. Biophys. Acta* **1971**, *227*, 429–441. (b) Odake, S.; Nakahashi, K.; Morikawa, T.; Takebe, S. *Chem. Pharm. Bull.* **1992**, *40*, 2764–2768.

(6) Todd, M. J.; Hausinger, R. P. *J. Biol. Chem.* **1989**, *264*, 15835–15842.

(7) X-ray parameters for $[\text{Ni}_2(\text{Hshi})(\text{H}_2\text{shi})(\text{pyr})_4(\text{OAc})]$: orthorhombic ($P2_1P2_1P2_1$, No. 19); $a = 13.507(3)$ Å, $b = 16.232(3)$ Å, $c = 16.502(3)$ Å; $V = 3618(1)$ Å³; $Z = 4$; $d_{\text{calc}} = 1.46$ g/cm³; crystal dimensions (mm), $0.22 \times 0.26 \times 0.32$; μ for Mo $K\alpha = 11.01$ cm⁻¹; $T = 178$ K; Siemens R3 m/v diffractometer, equipped with LT-2. An empirical absorption correction was used. The structure was solved by direct methods and refined using the SHELXTL PLUS program on a VAXStation 3500. Hydrogen atoms were refined $F \geq 2\sigma(F)$. Scan range $5 < 2\theta < 52$; unique reflections = 6912, refined reflections 6419, number of parameters = 608, $R = 0.0482$, $R_w = 0.0509$. The structure, **1**, has an unusual hydrogen-bonding network throughout the crystal. One salicylhydroxamate is singly deprotonated, and the other is doubly deprotonated (N1, N2, and O1 are bound to hydrogen atoms whereas O4 is not). As a consequence there is a network of intermolecular hydrogen bonds between the phenolic proton of O1 and O4.

(8) Characterization for $[\text{Ni}_2(\text{Hshi})(\text{H}_2\text{shi})(\text{pyr})_4(\text{OAc})]$, **1**: Anal. Calcd (found) for $\text{C}_{36}\text{H}_{34}\text{N}_6\text{O}_8\text{Ni}_2$: C 54.32 (54.16), H 3.9 (4.3), N 10.56 (10.39), Ni 14.75 (14.5). An ESI mass spectrum of **1** showed a mass peak at 637 (30% base) and 558 (100%) which correspond to the loss of bound pyridine in MeOH. If the pyridine dissociates from the structure in CH_3CN , it can then act as base and further deprotonate the salicylhydroxamic acid and reorganize to form a metallacrown which is consistent with the ESI spectrum of **1** in CH_3CN (peaks at 893 and 448).

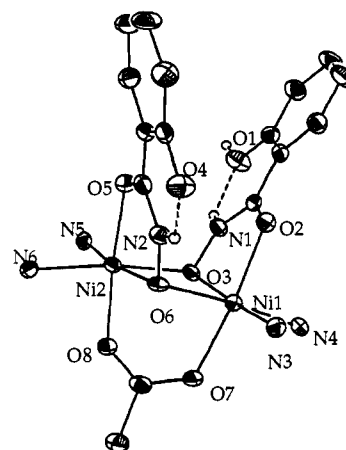
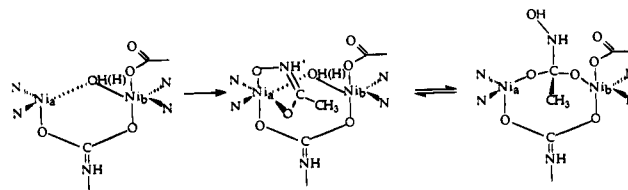


Figure 1. ORTEP diagram of $[\text{Ni}_2(\text{Hshi})(\text{H}_2\text{shi})(\text{pyr})_4(\text{OAc})]$ with thermal ellipsoids shown at 50% probability. Selected bond distances (Å): Ni1–O2 2.092(3), Ni1–O3 2.039(3), Ni1–O6 2.055(3), Ni1–O7 2.045(3), Ni2–O3 2.110(3), Ni2–O5 2.114(3), Ni2–O6 2.023(3), Ni2–O8 2.055(3). Selected bond angles (deg): O3–Ni1–O7 91.0(1), O3–Ni1–O6 85.6(1), O6–Ni1–O7 83.1(1), 95.2(1), O2–Ni1–O7 171.3(1), O6–Ni1–N3 88.8(1), O2–Ni1–O3 80.4(1), O3–Ni1–N3 172.0(1), O6–Ni1–N4 174.1(1), O3–Ni1–N4 91.7(1), O2–Ni1–O6, O2–Ni1–N3 94.5(1), O2–Ni1–N4 89.5(1), O7–Ni1–N3 94.0(1), O7–Ni1–N4 91.7(1), O3–Ni2–O5 97.2(1), O3–Ni2–O6 84.6(1), O3–Ni2–O8 83.2(1), O3–Ni2–N5 86.3(1), O3–Ni2–N6 171.6(1), O5–Ni2–O6 80.7(1), O5–Ni2–O8 168.2(1), O5–Ni2–N5 95.4(1), O5–Ni2–N6 90.3(1), O6–Ni2–O8 87.6(1), O6–Ni2–N5 169.5(1), O6–Ni2–N6 92.9(1), O8–Ni2–N5 96.4(1), O8–Ni2–N6 88.7(1), N3–Ni1–N4 94.4(1), N5–Ni2–N6 96.9(1), Ni1–O3–Ni2 93.2(1), Ni1–O6–Ni2 95.4(1).

Scheme 1



The nickel dimer $[\text{Ni}_2(\text{Hshi})(\text{H}_2\text{shi})(\text{pyr})_4(\text{OAc})]$, **1**, was synthesized by the reaction of 1.24 g (5mmol) of nickel(II) acetate tetrahydrate with 0.77 g (5 mmol) of salicylhydroxamic acid in 50 mL of methanol followed by the addition of 4 mL of pyridine. The solution was stirred for 2 h and then filtered. A 73% yield of green-blue crystals of **1** suitable for X-ray analysis formed after the solution was left to stand at low temperature for several days.^{7,8} An ORTEP diagram of **1** is shown as Figure 1. Similar to the native urease, this structure has two nitrogen atoms (from pyridine molecules) bound to each nickel and a bridging acetate. In addition there are two bridging, bidentate salicylhydroxamate molecules. The average Ni–N/O distance is 2.07(3) Å, which is similar to the 2.06 Å average distance found by EXAFS in native urease.⁹ The Ni–Ni distance for the hydroxamate-inhibited urease is unknown; however, β -mercaptoethanol-inhibited urease has the metals separated by 3.26 Å according to EXAFS studies.¹⁰ The Ni–Ni distance in **1** is 3.016 Å. This exceptionally short distance is a result of a triply bridging system which has two single-atom bridges (hydroxamate oxygens, O3 and O6) and one acetate bridge. *Since urease is inhibited stoichiometrically by hydroxamates, we suggest that the inhibited urease would only have one bridging*

(9) Clark, P. A.; Wilcox, D. E.; Scott, R. A. *Inorg. Chem.* **1990**, *29*, 579–581.

(10) Wang, S.; Lee, M. H.; Hausinger, R. P.; Clark, P. A.; Wilcox, D. E.; Scott, R. A. *Inorg. Chem.* **1994**, *33*, 1589–1593.

hydroxamate, which would lead to a greater Ni–Ni separation. Longer Ni–Ni separations are found with models^{11,12} that have one single-atom bridge.

In order to assess the magnetic exchange in this dimer, the solid state, variable temperature magnetic susceptibility of complex **1** was measured in an applied field of 0.5 T. The Heisenberg–Dirac–VanVleck Hamiltonian describing the exchange interaction between two octahedral Ni(II) ($S_1 = S_2 = 1$) centers is given by $\mathcal{H} = -2JS_1 \cdot S_2$. The energies of the corresponding states in the coupled representation, $|S_T, M_S\rangle$, (where S_T assumes values ranging from $S_1 + S_2$ to $|S_1 - S_2|$) are given by $E_{S_T} = -J[S_T(S_T + 1) - 4]$. This results in a singlet state at $E_{S_T=0} = 0$, a triplet at $E_{S_T=1} = -2J$, and a quintet at $E_{S_T=2} = -6J$. Zero-field splitting within each individual total spin multiplet was accommodated¹³ by operating on the $|S_T, M_S\rangle$ basis with the following Hamiltonian:

$$\mathcal{H}_{ZFS} = D_{S_T} \left[S_z^2 - \frac{1}{3} S_T(S_T + 1) \right]$$

The magnetic susceptibility and effective magnetic moment were fitted independently of one another and gave the following results for the spin Hamiltonian parameters: g (2.23 to 2.26), J (+4.68 to +3.87 cm^{-1}) and $D_{\text{Ni(II)}}$ (+0.30 to +0.45 cm^{-1}). The best fitted g values are consistent with g values reported for most nickel ions in an octahedral geometry ($g = 2.1$ – 2.3). The exchange interaction between Ni ions is found to be weakly ferromagnetic, resulting in an $S_T = 2$ ground state which is zero-field split with the $|2,0\rangle$ state lying lowest in energy. It is this zero-field splitting which causes the reduction of μ_{eff} at temperatures below 6 K. The room-temperature magnetic moment of 3.26 μ_B per nickel atom is consistent with the $3.39 \pm 0.12 \mu_B$ per nickel for the acetohydroxamic acid inhibited urease.^{4a}

Complex **1** is the only crystallographically characterized example of a hydroxamate bound to nickel in a bidentate fashion through the hydroxamate and carbonyl oxygens. The structure of bis(glycinohydroxamato)nickel(II) has been published,¹⁴ yet it involved coordination of the nitrogen, not the hydroxamate oxygen. The five-membered chelate involving the two oxygen atoms is much more common, having especially high binding constants to Fe^{+3} .¹⁵ Structure **1** is also unique in that the hydroxamate oxygen bridges the two nickel atoms. While dimeric oxime complexes have been known for some time,¹⁶ this type of bidentate bridging to transition metals through the hydroxamate oxygen has only recently been seen.¹⁷ Cognizant of this alternative mode of binding for hydroxamates, one may reevaluate the mechanism of urease inhibition by acetohydroxamic acid.

The most recently suggested model for the inhibition of urease involves the bidentate coordination of a hydroxamate followed

(11) Wages, H. E.; Taft, K. L.; Lippard, S. J. *Inorg. Chem.* **1993**, *32*, 4985–4987.

(12) (a) Buchanan, R. M.; Mashuta, M. S.; Oberhausen, K. J.; Richardson, J. F.; Li, Q.; Hendrickson, D. N. *J. Am. Chem. Soc.* **1989**, *111*, 4497–4498. (b) Chaudhuri, P.; Küppers, H.-J.; Wieghardt, K.; Gehring, S.; Haase, W.; Nuber, B.; Weiss, J. *J. Chem. Soc., Dalton Trans.* **1988**, 1367–1370.

(13) This strong exchange limit approach is valid when the exchange splitting between total spin multiplets is much greater than the zero-field splitting within a given multiplet. It is convenient to relate the zero-field splitting parameters within the coupled basis (D_{S_T}) to the single-site $D_{\text{Ni(II)}}$ using tensor operator methods. This results in the following relations: $D_{S_T=1} = -D_{\text{Ni(II)}}$ and $D_{S_T=2} = \frac{1}{3}D_{\text{Ni(II)}}$. [(a) Scaringe, R. P.; Hodgson, D. J.; Hatfield, W. E. *Mol. Phys.* **1978**, *35*, 701. (b) Bencini, A.; Gatteschi, D. *EPR of Exchange Coupled Systems*; Springer-Verlag: Berlin, 1990; pp 48–85.]

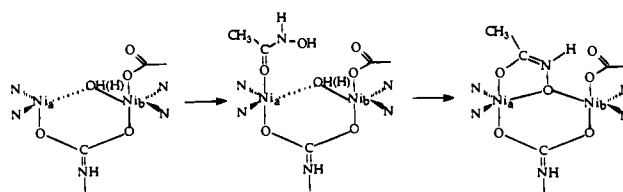
(14) (a) Brown, D. A.; Roche, A. L.; Pakkanen, T. A.; Pakkanen, T. T.; Smolander, K. *J. Chem. Soc., Chem. Commun.* **1982**, 3035. (b) Pakkanen, T. T.; Pakkanen, T. A.; Smolander, K.; Brown, D. A.; Glass, W. K.; Roche, A. L. *J. Mol. Struct.* **1987**, *162*, 313–320.

(15) Raymond, K. N.; Carrano, C. J. *Acc. Chem. Res.* **1979**, *12*, 183.

(16) (a) Ruiz, R.; Sanz, J.; Lloret, F.; Julve, M.; Faus, J.; Bois, C.; Muñoz, M. C. *J. Chem. Soc., Dalton Trans.* **1993**, 3035–3039. (b) Wu, Z.; Zhou, X.; Zhang, W.; Xu, Z.; You, X.; Huang, X. *J. Chem. Soc., Chem. Commun.* **1994**, 7, 813–814.

(17) (a) Lah, M. S.; Pecoraro, V. L. *Comments Inorg. Chem.* **1990**, *11*, 59. (b) Gibney, B. R.; Stemmler, A. J.; Pilotek, S.; Kampf, J. W.; Pecoraro, V. L. *Inorg. Chem.* **1993**, *32*, 6008–6015. (c) Gibney, B. R.; Kampf, J. W.; Kessissiglou, D. P.; Pecoraro, V. L. *Inorg. Chem.* **1994**, *33*, 4840.

Scheme 2



by a second, more stable complex, which involves the nucleophilic attack of hydroxyl ion bound to the second nickel atom.⁶ Scheme 1 incorporates the four histidine nitrogen donors, a bridging carbamate, a monodentate carboxylate from an aspartate residue, and a bound water (or hydroxide).³ The acetohydroxamic acid binds to one of the nickel atoms and then forms a tetrahedral intermediate analogous to the intermediate proposed for the decomposition of urea to carbonic acid and ammonia. With the recognition of the bridging mode found in complex **1**, an alternative series of inhibited states may be envisioned. The first, more weakly and more reversibly bound form would be that of the liganded monodentate carbonyl oxygen that is analogous to the model recently published by Lippard¹¹ for urea bound to nickel. The second, base dependent step would involve the hydroxamate being further deprotonated to allow the oxime oxygen to bind as the bidentate chelate and simultaneously bridge to the second nickel, atom shown in Scheme 2. With the exception of the second bridging hydroxamate oxygen atom, **1** has a nearly identical structure to this proposed enzyme form. Furthermore, the magnetic moment of the inhibited urease is consistent with the later structure shown in Scheme 2. Two crystal structures of enolase inhibited by phosphonoacetohydroxamate show differing binding modes of the hydroxamate.¹⁸ This diversity, coupled with the absence of a phosphono oxygen donor atom to orient the inhibitor, suggests that the binding of a simple hydroxamate has a third possible mode of binding, namely, the bridging, bidentate coordination found in complex **1**.

In conclusion, the structure of a nickel hydroxamate complex is presented which gives new insight for the mechanism of hydroxamate-based inhibition of dinuclear hydrolytic enzymes. These results show that the possibility of a hydroxamate bridging the two nickel atoms in urease is reasonable and that the properties of such an inhibited form are consistent with the accumulated physical data. Furthermore, as illustrated by enolase and aminopeptidases,¹⁹ inhibition of enzymes with dinuclear active centers by hydroxamates may generally rely on such bridging structures.

Acknowledgment. We would like to thank P. A. Karplus and R. P. Hausinger for allowing us to quote their unpublished results on the crystal structure of urease. This work was supported by the Sloan Foundation.

Supplementary Material Available: Plot of the magnetic susceptibility and effective magnetic moment versus temperature, ORTEP diagram depicting all numbered atoms, and tables of crystal parameters, atomic coordinates and selected bond lengths and angles, and isotropic and anisotropic thermal parameters (16 pages); observed and calculated structure factors (25 pages). This material is contained in many libraries on microfiche, immediately follows this article in the microfilm version of the journal, can be ordered from the ACS, and can be downloaded from the Internet; see any current masthead page for ordering information and Internet access instructions.

JA950466V

(18) (a) Wedekind, J. E.; Poyner, R. R.; Reed, G. H.; Rayment, I. *Biochemistry* **1994**, *33*, 9333–9342. (b) Zhang, E.; Hatada, M.; Brewer, J. M.; Lebioda, L. *Biochemistry* **1994**, *33*, 6295–6300. Reference 18b shows only the hydroxamate oxime oxygen bound in a nonbridging fashion. Reference 18a shows that the bridging heteroatom is the carbonyl oxygen; however, an oxime oxygen bridge could be envisioned for acetohydroxamate since it does not have the restriction of a phosphono oxygen binding site that conformationally enforces a carbonyl bridge.

(19) Wilkes, S. H.; Prescott, J. M. *J. Biol. Chem.* **1983**, *258*, 13517–13521.